



Exploration of Near-Term Urban Air Mobility Operations with Retrofitted Electric General Aviation Aircraft

Mark T. Kotwicz Heniczek,* Andrea Garbo,† Mark Lau,‡ Brian J. German,§ and Laurie A. Garrow¶
Georgia Institute of Technology, Atlanta, GA, 30332, U.S.A.

Urban Air Mobility (UAM) is rapidly gaining consumer and investor interest but faces a number of challenges that must be overcome. These challenges include battery technology, increasing levels of automation and autonomy, noise, vehicle certification, and airspace management. In this paper, we explore the potential of a near-term small-scale UAM service that avoids many of these challenges through the use of a currently available general aviation airplane retrofitted with an electric propulsion system. In particular, we investigate the applicability of a battery electric variant of the Cessna 208B Caravan for short-haul intracity commuter trips in U.S. cities. Missions with a range of up to 50 nautical miles at a cruise speed of 150 kts are anticipated to be feasible using current battery technology. Based on the opportunity to reduce passenger commuting time compared to driving, we find that in certain U.S. cities with geographic constraints and high levels of traffic congestion, there is significant potential demand for such a service, even considering the first- and last-mile challenges of trips to and from origin and destination airports. This type of UAM service might be a useful initial step as a “minimum viable product” to assess the public’s willingness to adopt aviation for short ranged daily trips if the price point of the service can be reduced adequately via new technologies such as electric propulsion.

Nomenclature

C_{batt}	battery capacity	ω_{batt}	battery derating factor
\dot{c}	battery C-rate	Δt_{ij}	time saved
E	energy	ϵ	battery pack specific energy
h	altitude	$\tau_{ij,air}$	flying time by air from airport to airport
\dot{h}	vertical climb speed		
k	aerodynamic/mission coefficient		
LD	lift to drag ratio		
P	power		
R	range		
$t_{i,car}$	driving time from household to airport	empty	empty
$t_{ij,car}$	driving time from household to workplace	flight	flight
$t_{j,car}$	driving time from workplace to airport	pass	passengers
t	time	res	reserve
V	flight speed	taround	turnaround
W	weight force [lbs] or [N]	tot	total

Subscripts

batt	battery
cl	climb
ch	charge
cr	cruise
empty	empty
flight	flight
pass	passengers
res	reserve
taround	turnaround
tot	total

I. Introduction

URBAN Air Mobility (UAM) has received considerable attention because of its potential to significantly reduce travel time by overflying ground congestion. UAM has seen several early iterations in the past decades, including helicopter charter services and regional corporate shuttle flights. Intracity air transport specifically has also been a topic of interest for several decades. A study by the MIT Flight Transportation Laboratory in 1970 [1], which investigated future urban transportation systems, identified inter-airport flights within cities as a likely future aviation market, while

*Graduate Research Assistant, Daniel Guggenheim School of Aerospace Engineering.

†Graduate Research Assistant, Daniel Guggenheim School of Aerospace Engineering.

‡Undergraduate Research Assistant, Daniel Guggenheim School of Aerospace Engineering.

§Associate Professor, Daniel Guggenheim School of Aerospace Engineering, AIAA Associate Fellow.

¶Professor, School of Civil and Environmental Engineering.

a study from 1952 by the Port of New York Authority identified intracity helicopter flights as an emerging mode of transportation [2]. Operation of intracity and inter-airport flights with helicopters has seen limited success due to high operating costs. Notable exceptions include New York City Airways, which operated Sikorsky helicopters from the roof of the Pan Am building in NYC from 1953 to 1979 [3] and more recently intracity and inter-airport operators BLADE, which operates in New York City and Los Angeles [4], and Voom, which operates in Sao Paulo, and Mexico City [5]. UAM has recently attracted a great deal of attention and investment due to the potential for recent advances in battery technology, distributed electric propulsion systems, and automation to dramatically reduce aircraft operating costs.

Significant technical hurdles remain, however, before electric-VTOL UAM can come to market. Battery technology remains immature with low charge rates, low capacity, and an unproven safety record. Important limitations also exist with the current Air Traffic Control (ATC) system that render it unsuitable for large scale UAM operations; increased levels of ATC automation are required before a large volume of UAM flights can operate safely. The noise signature of UAM aircraft is also a nontrivial issue due to the low-altitude operation of UAM over densely populated urban areas. Another significant hurdle is aircraft certification. Many of the aircraft designs now being proposed for UAM differ greatly from current aircraft, incorporating distributed electric propulsion and new forms of flight control, meaning that certification of these systems will require a significant effort.

These hurdles, in addition to large infrastructure development costs, land-use regulations, and uncertainty regarding the impact of increasing levels of autonomy, have left a number of important questions regarding the UAM market unanswered. Little is known regarding the logistics necessary to minimize aircraft-on-ground time, solutions for the first and last-mile problem associated with UAM remain untested, and the large estimates for the potential UAM market remain largely speculative. Suitable price points for profitability and inclusiveness of the general population remain unknown, and the feasibility of UAM operations from existing airports, particularly larger airports, is unclear. Important questions also remain regarding customer behavior [6]. For example, the willingness of customers to take public or private ground transportation during the first and last mile of the commute, the maximum departure delay customers are willing to accept, and the minimum time savings relative to conventional ground transportation necessary for customers to consider UAM as an attractive alternative remain uninvestigated. Furthermore, the percentage of potential customers willing to fly on small general aviation aircraft on a daily basis, the value customers place on cabin comfort, and lastly, the value customers place on time-saved and more specifically, time saved from being stuck in traffic without opportunity for productivity are also unknown.

Considering the many uncertainties and challenges along the pathway to at-scale UAM services with eVTOL aircraft, there may be value to implementing near-term trial services that offer the potential to test market opportunities. In this context, the use of existing general aviation aircraft, retrofitted with electric propulsion systems, may overcome many of the hurdles associated with certification of more complex eVTOL UAM vehicles. Furthermore, by using existing airports and introducing relatively few additional aircraft, additional infrastructure and special integration into the air traffic control system is not required. To evaluate the potential of such near-term UAM services this paper proposes the use of retrofitted Cessna 208B Grand Caravans to transport commuters between airports within a 50 nautical mile radius of major U.S. cities at a cruise speed of 150 kts. Evaluation of the potential demand for this type of UAM service is the primary focus of the manuscript. Demand is estimated by assessing the number of commuters who would save a substantial amount of time by using the service compared to driving.

The Cessna 208B Grand Caravan was selected for a number of reasons. The aircraft has seen over 30 years of service with a reliable reputation for high-frequency commercial operations [7]. Low cost, used Cessna 208B aircraft are widely available due to their popularity among operators and the 9-passenger capacity is appropriate for the anticipated demand and current state of battery technology. The cargo pod located on the bottom of fuselage could also be converted for battery storage without modifying the aerodynamic envelope of the aircraft and the turboprop engine could be replaced by an electric motor, potentially allowing for certification through a Supplemental Type Certificate (STC). Additionally, the Cessna Caravan is already being explored by several companies, including Magnix, for short-range pure electric operation [8].

Although electric VTOL has not yet been commercially realized, all-electric aircraft have been adopted by a number of companies such as Pipistrel and OSM Aviation for use as pilot training aircraft [9], and has spawned initiatives such as the Sustainable Aviation Project in California [10]. The feasibility of retrofitting general aviation aircraft with electric motors has previously been studied [11, 12], where it was concluded that only minimal range would be feasible without the introduction of novel aircraft concepts specifically designed for all-electric flight. Advances in battery technology, however, have already enabled the range capability of the proposed mission and has led Harbour Air, which operates the largest all seaplane fleet in North America, to announce (March 2019) plans to retrofit their entire seaplane fleet with electric powerplants, starting with the 6 passenger De Havilland Beaver [13]. Work on electric

aircraft motors is ongoing, with both small and large corporations including Siemens, MagniX, and Safran working to bring products to market. The notable research and industrial effort to develop electric propulsion motors for aircraft is primarily motivated by the significant reduction in operational cost associated with electric motors. OSM Aviation, for example, claims an 80% reduction in operational costs using the Bye Aerospace Eflyer compared to the Cessna 172, which it plans to phase out for their pilot training programs[14].

This paper demonstrates the technological feasibility of the proposed mission and seeks to provide preliminary information regarding market demand for short-haul intracity flights. The paper begins by describing the methodology used to explore the design space of a retrofitted Cessna 208B Grand Caravan and proceeds to detail the process used to identify regions and routes of interest on both a nationwide and citywide scale. Results for each of these topics are subsequently presented.

II. Methodology

In this section, we first describe the methodology used to estimate the lift-to-drag ratio and empty weight of the Cessna 208B Grand Caravan retrofitted with an electric motor–technical parameters necessary for the aircraft performance analysis. Next, the equations used to establish the maximum feasible range and cruise speed of the retrofitted aircraft are presented. Finally, the process for estimating the potential demand for the proposed service is described.

A. Retrofitted Cessna 208B Empty Weight and Lift-to-Drag Ratio

The lift-to-drag ratio curve of the Cessna 208B is estimated by combining drag polar results obtained via the OpenVSP software’s parasite drag tool along with maximum glide performance range data available in the pilot operating handbook [15]. The Cessna 208B OpenVSP model and the corresponding estimated lift-to-drag ratio curve are illustrated in Fig. 1.

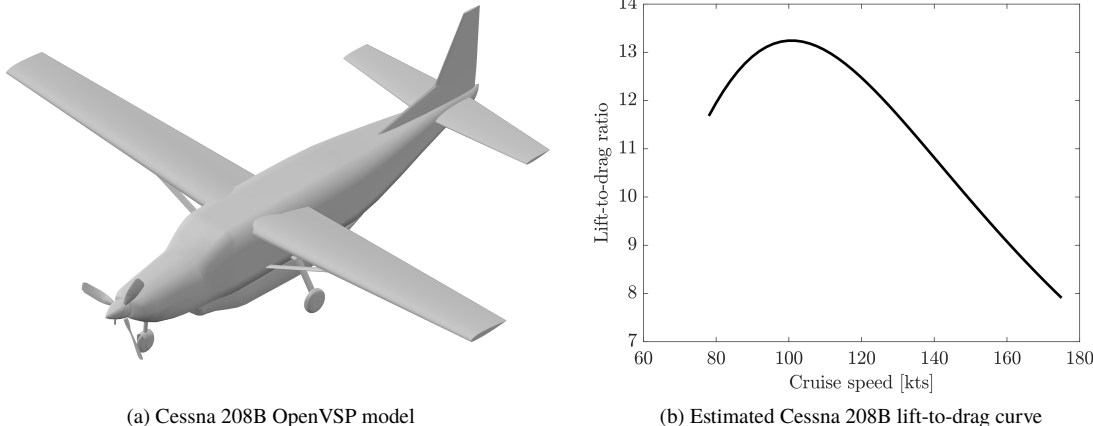


Fig. 1 Cessna 208B OpenVSP model and corresponding estimated lift-to-drag ratio curve.

The empty weight of the Cessna 208B (i.e. the aircraft weight excluding the passengers and battery) is obtained by first subtracting the weight of the original turboprop engine (360 lbs for the PT6A-114A [16]) from the original aircraft empty weight (4,511 lbs [15]). An estimation of the electric motor weight (168 lbs) is then added to estimate the new empty weight of the retrofitted Cessna 208B. The electric motor weight is estimated by dividing the PT6A-114A rated power of 675 hp by a specific power value for near-term technology electric motors of 4 hp/lb [17–19]. The empty weight of the retrofitted aircraft is then estimated as:

$$W_{\text{empty}} = 4,511 - 360 + 168 = 4,319 \text{ lbs} \quad (1)$$

To determine the maximum installed battery capacity of a retrofitted Cessna 208B, the analysis must take into consideration some constraints related to the aircraft structure, specifically the maximum landing weight, the maximum

cargo pod payload capacity, and the cargo pod internal volume, all of which are listed in the Cessna 208B pilot operating handbook, and have a values of 8,500 lbs, 1,090 lbs, and 111.5 ft³, respectively. Given the low maximum payload of the cargo pod relative to its internal volume, it was assumed that the cargo pod payload limit could feasibly be tripled to 3,270 lbs without a significant impact on the aircraft empty weight (e.g. using composite materials) and without affecting the integrity of the overall aircraft structure. Another way of interpreting this assumption is that any additional structural weight will be offset by a reduction in the allowable payload weight, i.e. the number of passengers, such that the landing weight remains fixed. This assumption was deemed reasonable due to the simple structural design of the original cargo pod. It should also be mentioned that the entirety of the battery pack is assumed to be stored in the cargo pod. Summarizing, the two aircraft constraints considered in this study are:

$$W < 8,500 \text{ lbs} \quad (2)$$

$$W_{\text{batt}} < 3,270 \text{ lbs} \quad (3)$$

B. Aircraft Performance Modeling

The mission profile considered in this analysis consists of climb and cruise phases in addition to a 30 minute reserve segment flown at maximum-range-speed to fulfill FAR 91.151 regulations [20]. The descent phase is considered as a no credit descent, and is therefore not included in the analysis. Aircraft performance is analyzed using an energy-based method, where the total energy required to complete the mission (E_{tot}) is obtained by summing the energy required during climb (E_{cl}), cruise (E_{cr}), and reserve (E_{res}) phases. More formally:

$$E_{\text{tot}} = E_{\text{cl}} + E_{\text{cr}} + E_{\text{res}} \quad (4)$$

$$E_{\text{cl}} = W \left(\frac{V_{\text{cl}}}{\text{LD}_{\text{cl}}} + \dot{h} \right) \frac{\Delta h}{\dot{h}} \quad (5)$$

$$E_{\text{cr}} = \frac{W}{\text{LD}_{\text{cr}}} (R - R_{\text{cl}}) \quad (6)$$

$$E_{\text{res}} = \left(\frac{W}{\text{LD}_{\text{max}}} V_{\text{LD},\text{max}} \right) t_{\text{res}} \quad (7)$$

where W is the total aircraft weight, Δh is the altitude gain during the climb phase, \dot{h} is the vertical climb speed, V_{cl} is aircraft speed during climb, $V_{\text{LD},\text{max}}$ is the speed corresponding to the maximum lift-to-drag ratio value (LD_{max}), R is the total mission range, R_{cl} is the range portion completed during the climb phase (i.e. $V_{\text{cl}} \cdot \Delta h / \dot{h}$), t_{res} is the reserve time (30 minutes as indicated in FAA regulations [20]), and LD_{cl} and LD_{cr} are the lift-to-drag ratios at climb and cruise speed, respectively. Combining Eq. (4) with Eq. (7), it is possible to obtain:

$$E_{\text{tot}} = W \left(\left(\frac{V_{\text{cl}}}{\text{LD}_{\text{cl}}} + \dot{h} \right) \frac{\Delta h}{\dot{h}} + \frac{1}{\text{LD}_{\text{cr}}} (R - R_{\text{cl}}) + \frac{V_{\text{LD},\text{max}}}{\text{LD}_{\text{max}}} t_{\text{res}} \right) \quad (8)$$

$$= Wk \quad (9)$$

where the coefficient k depends only on mission profile and aircraft aerodynamic characteristics. E_{tot} and W are not independent since the total aircraft weight is a function of the battery weight, which in turn, is a function of the energy required to complete the mission. More specifically:

$$W = W_{\text{empty}} + W_{\text{pass}} + W_{\text{batt}} \quad (10)$$

$$W_{\text{batt}} = \frac{E_{\text{tot}}}{\omega_{\text{batt}} \epsilon} \quad (11)$$

where W_{empty} is the empty weight, W_{pass} is the passenger weight, W_{batt} is the battery pack weight, ϵ is the battery pack specific energy, and ω_{batt} is a battery capacity derating factor used to take the non-linear behavior of battery cells into consideration. Finally, combining Eq. (11) with Eq. (8), the total amount of energy required to complete the mission can be estimated as:

$$E_{\text{tot}} = (W_{\text{empty}} + W_{\text{pass}}) \frac{k}{1 - \frac{k}{\omega_{\text{batt}} \epsilon}} \quad (12)$$

Eq. (12) is a first-order approximation of the amount of energy required by an electric aircraft to complete a prescribed mission considering a certain battery technology level (i.e. ω_{batt} and ϵ). Once E_{tot} is estimated, the total aircraft weight can be calculated using Eq. (10) and Eq. (11). Although the above methodology relies on several simplifying assumptions, it is capable of establishing reasonable values of range and cruise speed for the proposed urban air mobility mission.

C. Estimation of Anticipated Demand

Anticipated demand for the proposed mission is characterized using two metrics: the number of potential customers that would benefit from the proposed mission and the value proposition of the mission itself, measured by the amount of time customers save by using the service relative to commuting using the road network. Both are estimated using the Longitudinal employer-household dynamics Origin-Destination Employment Statistics (LODES) dataset. The LODES dataset consists of worker demographics information and economic indicators, including household and workplace location information at the census block level. Due to the fine-grained geographic resolution of census blocks, geographical coordinates for each household-workplace origin-destination (OD) pair can be entered into a mapping service to estimate commuting distance and duration. The American Community Survey (ACS) dataset, which provides detailed population and housing information at the census tract level, is used in conjunction with the LODES data to estimate the fraction of customers who are single drivers and earn above \$75,000 annually, and are hence more likely to be able to afford and to benefit from a near-term UAM service. Other potential metrics that may be of interest from the standpoint of demand estimation, such as the time saved per mile or the total value of a region (which could be approximated by multiplying an assumed value for time saved by the number of potential customers) were not utilized to maintain simplicity and transparency of results.

In order to estimate the time commuters save by using the service, each work and home location from the LODES data is linked to the nearest public airport (in terms of driving duration) via the publicly available *OurAirports* dataset [21]. Time savings can then be calculated by comparing the driving time between each workplace and household pair to the total trip duration of the corresponding UAM mission, i.e. driving from home to the nearest airport, flying to the work airport, and driving to work. More formally, time savings, Δt_{ij} , can be written as:

$$\Delta t_{ij} = t_{ij,\text{car}} - (t_{i,\text{car}} + \tau_{ij,\text{air}} + t_{j,\text{car}}) \quad (13)$$

where $t_{ij,\text{car}}$ is the commuting time driving from the i^{th} to the j^{th} census block, $t_{i,\text{car}}$ is the time taken to drive from the i^{th} census block to the nearest airport, $\tau_{ij,\text{air}}$ is the flying time between the household-workplace associated airports, and $t_{j,\text{car}}$ is the time taken to drive from j^{th} census block to the nearest airport. The travel distance between airports is computed using the haversine distance formula, from which the airport-airport travel time is calculated assuming an average aircraft speed of 150 kts. The distance traversed through the road network serving the same household-workplace pair was approximated using the Open Source Routing Machine (OSRM) engine, while the travel duration, on the other hand, is computed differently based on the scale of the analysis, as described in Sections II.C.2 and II.C.3. All routes with common origin and destination airports can then be grouped to evaluate the number of customers served by each airport pair and the associated average time saved across all potential customers—the two metrics used to estimate the potential demand.

A series of filtering steps are used to remove undesirable origin-destination pairs from the dataset, which also improves computational speed during analysis of the data by decreasing the size of the dataset. Filtering criteria include limiting the flyover distance between airports to 50 nmi, limiting the household-airport and workplace-airport haversine distance to 100 km, removing routes with time savings under 30 minutes, and removing airport pairs whose catchment areas serve less than 100 residents. The airport dataset is also filtered, such that only public, on-ground airports are considered. Seaplane ports, heliports, and closed airports are removed from the dataset as they were not suitable for operation of the Cessna Caravan chosen for the proposed mission. Furthermore, the states of Alaska and Hawaii were not considered due to limited road network connectivity in road maps used by OSRM for those regions.

1. Assumptions

A number of important assumptions are made during the nationwide and citywide analysis. First, the home and destination locations of the LODES data are assumed to accurately represent origin-destination pairs used by commuters on a daily basis. The exact coordinates of the origin and destination pairs are assumed to be at the centroid of their respective census blocks. Second, potential demand was estimated purely based on the commuting data available from the LODES dataset. As such, the approach does not account for demand associated with leisure trips and other

trip purposes. Finally, it should be noted that all delays, including those related to transitions between modes of transportation, taxiing time, and delays associated with obtaining takeoff clearance are not modeled at present. However, these delays must be taken into consideration when interpreting the results for time savings presented in this paper.

2. Nationwide Analysis of Favorable Areas of Operation

The purpose of the nationwide-level search is to quickly assess a large number of routes across the U.S. and to present several approximate metrics that, when combined, can be used to judge an overall geographic region's suitability for the proposed near-term mission. The results of this search are intended to be used to guide the selection of specific cities on which a more detailed analysis, described in Section II.C.3, is applied in order to identify specific routes of interest.

In order to make the analysis feasible, a number of additional simplifications and assumptions are made. Most notably, the commuting demand for the nationwide analysis is expressed in terms of OD pairs of census block groups rather than individual census blocks. To further reduce the dataset under consideration, only trips between home and work locations within a haversine distance of 10 nmi of at least one airport are considered and trips within the LODES dataset crossing state boundaries are omitted. It should also be noted that LODES implied trips with time savings greater than 3 hours are removed in order to reduce the number of outlier routes that result from OSRM's tendency to overestimate travel times for certain routes that involve utilization of a car ferry service. This filtering improves the ability of each heatmap to present meaningful results relevant to the mission. Additionally, the car travel time between the household, workplace, and their respective closest airports are approximated using OSRM with a 50% time penalty applied to approximate rush hour traffic congestion. Omission of an accurate traffic layer at the national scale is acceptable since routes that will ultimately be of interest will feature both heavy congestion and have road network distances that are significantly longer than the overflight distance, the latter of which can be detected without traffic information.

3. Citywide Analysis of Favorable Airport Pairs

The citywide analysis for favorable airport pairs follows much of the same methodology and logic as the nationwide analysis with the important exception of the addition of a traffic layer. As described above, the analysis relies on LODES commuter data to extract home-work pairs, each of which is assigned a home and work airport, based on minimizing travel time. Instead of applying a 50% traffic penalty to routes computed with the OSRM engine, however, the Google Maps Traffic API is used to generate an approximate traffic matrix for each city of interest. This is done by using the traffic API to calculate the average vehicle speed between every possible combination of a non-uniform grid of points during peak traffic hours. Traffic data corresponding to the OD pairs that most closely match the routes of interest is used in conjunction with the driving distance between home, work, and airport locations (calculated using the OSRM engine) to estimate trip duration.

A custom grid is used for each city to avoid grid vertices being placed in non-residential or non-commercial areas. Only approximately 100 points are queried for traffic information per city given that N points requires $\frac{N!}{2(N-2)!}$ API calls. Traffic in each direction between two vertices is assumed to be identical to reduce the number of calls needed. Routes which rank highly based the metrics for anticipated demand are called individually using the traffic API to increase the fidelity of the traffic data utilized. The 'best guess' option and a fixed future workday (non-weekend) is used within the API during traffic grid generation. Peak traffic hours are assumed to be 5:00 PM for each city considered. It should be noted that the route path used by OSRM to calculate distance is assumed to be the same as the path selected by the Google traffic API, used to estimate the average driving speed. This leads to potential errors in the estimation of time savings for a small number of cases where the route used to estimate traffic is significantly different to the route used to calculate distance in terms of distance or congestion.

To avoid the interaction of neighbouring airports, once the top ranked airport pairs have been identified in a region, each home and work location in the LODES data is reassigned to one of the aforementioned top-ranked airports and the analysis is repeated. This ensures that the catchment zone of the selected airports is not being affected by a nearby secondary airport, which, in the initial citywide analysis, may have served a number of customers that also fall within the catchment zone of the higher-ranked airport. The number of considered airport pairs can be varied depending on the objective of the analysis. The potential customer base and the associated time savings of each airport pair contributes to the suitability of a city as a host for the proposed mission. The city with the most advantageous combination of time-savings and number of customers served is deemed most suitable. Given that the importance of the number of customers relative to the associated time saved is unknown, the two metrics are presented in a decoupled manner to avoid loss of information.

4. Important Factors Not Included in Analysis

A number of important factors that impact the suitability of a city or airport pair for the proposed mission are not considered to avoid the introduction of incomplete data sets or subjective criteria. Nevertheless, upon interpretation of the included results, the following factors should be considered.

- Local weather patterns and their effect on VFR (visual flight rules) operation
- ATC and airport capacity
- Local air traffic congestion
- Existing electrical power infrastructure at airports of interest
- Available methods of public transportation along commuter routes

III. Results

The aircraft performance results used to guide the selection of a 50 nmi range and 150 kts cruise speed for the proposed mission are detailed below. Results illustrating nationwide and city-specific demand are subsequently presented.

A. Aircraft Performance Characteristics

The performance of the electric retrofitted Cessna 208B Grand Caravan is explored in Fig. 2 using the equations presented in Section II.B and the values listed in Table 1.

Table 1 Assumed values for Cessna 208B performance analysis.

Variable	Value
\dot{h}	1,000 ft/min [15]
Δh	3,000 ft
t_{res}	30 min
ω_{batt}	0.8 [22]
ϵ	200 Wh/kg

Fig. 2 shows the aircraft weight as a function of mission range and cruise speed assuming a loading of 7, 8 and 9 passengers. The black and red hatched lines represent the maximum landing weight and maximum battery weight constraints, formulated in Eq. (2) and Eq. (3), respectively. As expected, the feasible region shrinks as more passengers are loaded in the aircraft due to a decrease in the portion of the aircraft weight that can be allocated to the battery pack. Interestingly, the maximum aircraft weight is the binding constraint, meaning that tripling the weight-bearing limit of the cargo-pod is excessive, and less structural reinforcement might be necessary to successfully complete the proposed mission.

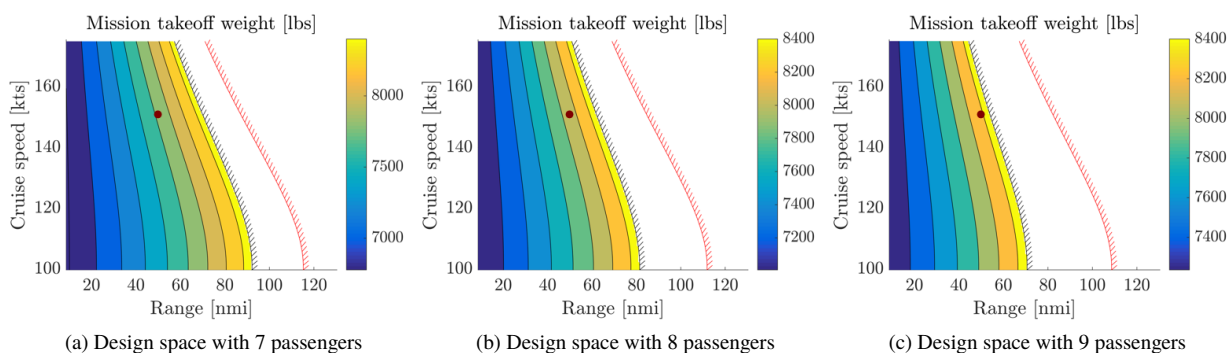


Fig. 2 Takeoff weight of the retrofitted Cessna 208B as a function of range and cruise speed for three different numbers of passengers. The red dot indicates the mission range and cruise speed values used in this study.

As can be observed from Fig. 2, a range of 50 nmi at a cruise speed of 150 kts is feasible with some margin for error, even with 9 passengers on board.

The turnaround time, important for the operation of electric aircraft and therefore necessary to demonstrate mission feasibility, can be estimated as the sum of flight and charging times:

$$t_{\text{taround}} = t_{\text{ch}} + t_{\text{flight}} \quad (14)$$

$$t_{\text{ch}} = \frac{E_{\text{tot}}}{\max(\dot{c}_{\text{ch}} C_{\text{batt}}, P_{\text{ch}})} \quad (15)$$

$$t_{\text{flight}} = \frac{\Delta h}{h} + \frac{R - R_{\text{cl}}}{V_{\text{cr}}} \quad (16)$$

where \dot{c}_{ch} is the charging c-rate, C_{batt} is the battery capacity, and P_{ch} is the maximum power available at the charger. Fig. 3 shows t_{flight} , t_{ch} , and t_{taround} for the nine passenger configuration, $\dot{c}_{\text{ch}} = 1$, and $P_{\text{ch}} = 300 \text{ kW}$. As expected, the charging time is a sizeable fraction of the turnaround time and has roughly the same order of magnitude of the flight time. The turnaround time for the proposed mission is approximately 50 minutes, meaning that two commuting flights are possible within a three hour rush period. Although turnaround times of this magnitude are high relative to fuel-burning aircraft, faster times for electric aircraft are not possible without advances in charger technology. It should be noted that these time estimates do not account for additional ground wait time not associated with battery recharging such as en-route delay times related to air traffic control considerations.

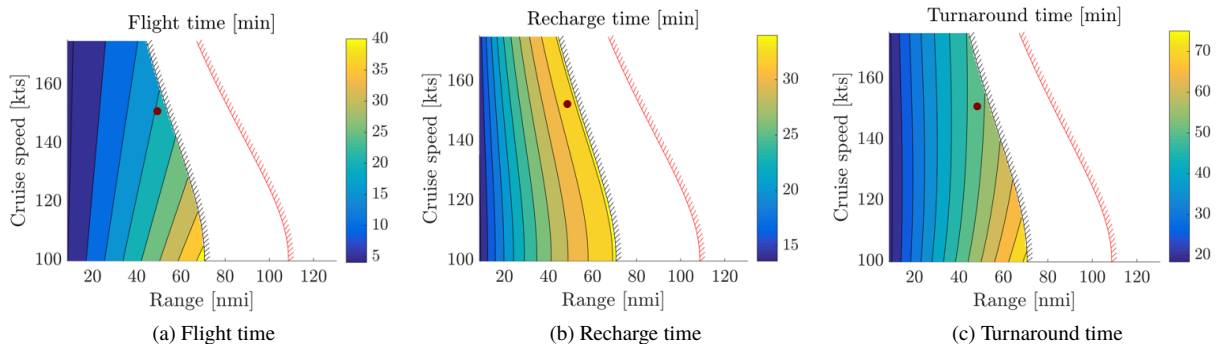


Fig. 3 Mission time, recharge time, and turnaround time as a function of range and cruise speed for a retrofitted Cessna 208B with 9 passengers.

The above results, combined with the demand and route analysis described in the following sections form the basis of the feasibility hypothesis for the proposed mission.

B. Nationwide Results

Estimated anticipated demand for the proposed mission at the national scale is presented in Figs. 4 and 5. Heatmaps are used to present the results to enable quick identification of regions of interest based on the two metrics described previously: the total number of potential customers and the average potential time savings of customers using the service. Hence, the heat-maps below measure both the concentration (number of viable airport pairs in a given region) and the intensity (performance of individual airport pairs based on the metrics of interest) of routes in the area, which when combined, are assumed to suggest a higher probability that suitable routes exist within a given region.

A limitation of keeping the two aforementioned metrics separate is that the desired simultaneity of the metrics is not captured. For example, a region may contain several airport pairs that have the potential to serve a large number of customers but have very low associated time savings while also containing several airport pairs with large associated time savings but very small catchment areas. In other words, if the metrics are kept uncoupled there is no guarantee that a particular airport pair within a region scores well on both metrics.

The use of a composite metric synthesized from the two metrics may partially solve the problem, but due to the dissimilar nature of each measure, a simple multiplication of the two is not suitable. To avoid the introduction of an

arbitrary combined metric, a series of heatmaps is used, with each heatmap populated only with routes satisfying a filter requiring increasing minimum time saved per route and a minimum number of potential customers (Fig. 4a, for example, represents routes which serve a minimum of 100 passengers and have a minimum of 30 minutes time savings; Fig. 4f represents routes which serve a minimum of 1,000 passengers and have a minimum of 50 minutes time savings). Each route is represented as a point on the map, with regions that contain dense clusters of points rendered as red spots. Each heatmap measures both the relative densities of favorable routes across the nation as well as the quality of the routes themselves, where the quality of routes is characterized by the number of potential customers per airport route for heatmaps on the left-hand column of Fig. 4 and by the associated time savings for heatmaps on the right-hand column of Fig. 4.

The trend displayed by this set of results gives a strong indication of regions that contain a high density of routes that are able to serve a large customer base while also providing substantial time savings. Due to the nature of heatmaps, low density regions that satisfy both metrics, such as regions with a single route that has significant time savings and serves a large number of customers, are not identified in the presented results.

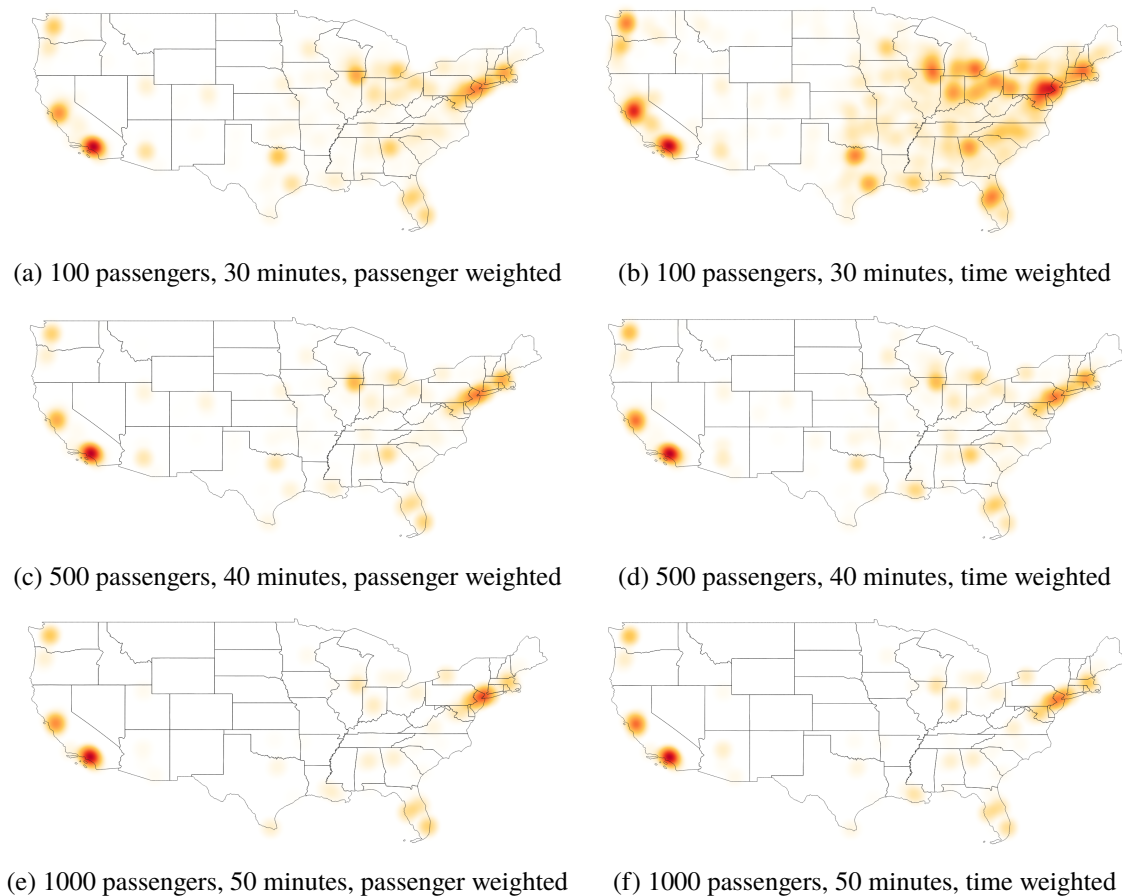


Fig. 4 Heatmaps of potential passengers and average time saved.

As expected, higher concentrations of routes with large numbers of potential customers are focused around city centers likely due to the inherently increased population size and densities. This is observed to be the case in high-density cities such as New York and Los Angeles. Routes that have higher time savings, on the other hand, tend to occur where the overflight distance is significantly shorter than the road network. For this reason, regions with large bodies of water separating populated areas, particularly those that rely on ferry services such as Seattle, have significant time savings. It should also be noted that there is an inherent coupling between the two columns of heatmaps, which is responsible, in part, for their similarity to one another: heatmap coloring is based both on route quality and route density. Areas that

feature a much larger number of routes have a much higher chance of containing airport pairs that have both a large potential customer base and strong associated time savings. High population density areas also tend to feature increased road congestion which leads to larger time savings and hence larger catchment areas, which again increases the number of potential customers. Since traffic is not predicted in the nationwide analysis, however, the latter coupling effect is not present.

Heatmaps for routes with passenger numbers scaled by the fraction of individuals with an income of more than \$75,000 who drive to work without carpooling (derived from the ACS dataset) is also presented. Due to the reduced number of potential customers that meet these requirements upon the introduction of the ACS data, the requirements for the minimum number of passengers per airport pair is reduced by an order of magnitude.

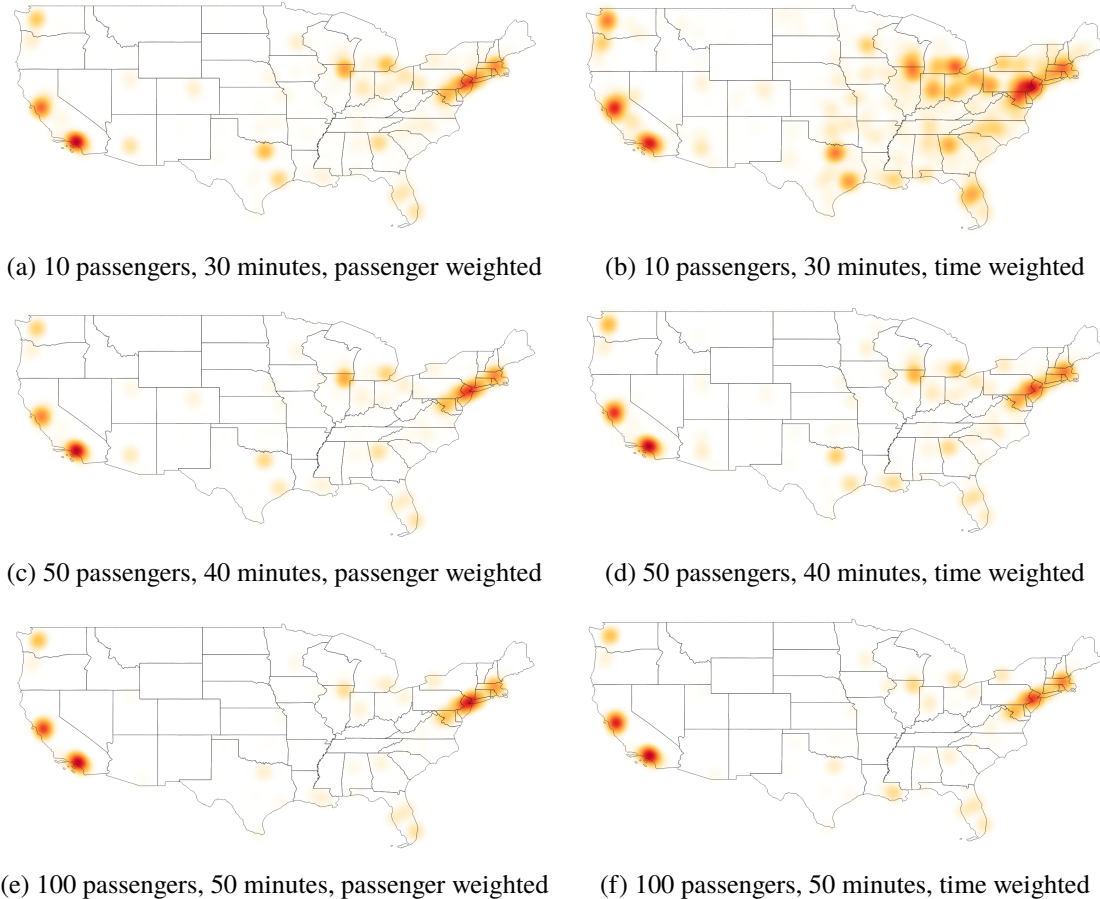


Fig. 5 Heatmaps of potential passengers and average time saved weighted with consideration of ACS data.

Differences between heatmaps with and without ACS data are small, although New York City and San Francisco appear brighter and more favorable relative to the rest of the nation in the second, third, and fourth rows of Fig. 5 than compared to in the same rows of Fig. 4. This suggests that a greater fraction of the populations in these two cities earn yearly incomes greater than \$75,000 and commute to work by car. However, as the effects of this difference is small, the results of the nationwide analysis and the selection of cities for further analysis was insensitive to differences in this fraction across the nation.

From Figs. 4 and 5, the cities of Los Angeles, San Francisco, and New York City are noticeably dominant under both metrics, with and without ACS data. In addition, Seattle and Chicago, although not as dominant, continue to appear in several heatmaps with increased constraints. This suggests that these cities are suitable for further analysis at the citywide scale and imply that the search for suitable routes using traffic layers can be narrowed to these cities due to a high probability that favorable routes can be found.

While these results are not particularly surprising, Chicago and New York City appear to be less favorable relative to Los Angeles than expected. This may be attributed a large number of potentially favorable routes being interstate trips, which are not factored into the nationwide analysis because of the difficulty of merging the different datasets which are organized by state. Bright spots corresponding to the cities of New York and Chicago on each heatmap are observed to cross state boundaries, suggesting that these cities would have likely appeared more favorable had interstate routes been factored in. Although the presented nationwide analysis relies on a number of simplifying assumptions, the fundamental nature of the method (identifying routes where the road network distance is larger than the overflight distance) lends credibility to the results and yields potential locations of UAM operations that are in line with previous studies under different metrics than the ones used within this paper [23].

C. Citywide Results

Based on the nationwide analysis of the anticipated demand, the cities of Seattle, San Francisco, Los Angeles, Chicago, and New York were selected to be analyzed with greater detail. Results for the aforementioned cities are presented in Fig. 6, where the x-axis denotes the number of potential customers served by each airport pair and the y-axis demonstrates the average time savings of those customers. All possible airport pairs that serve a minimum of 1,000 customers, with each OD pair having a minimum time savings of 40 minutes are included in Fig. 6. For this reason, the number of data points vary per city. Chicago, for example, has a larger number of airport pairs that adhere to the chosen criteria relative to Seattle.

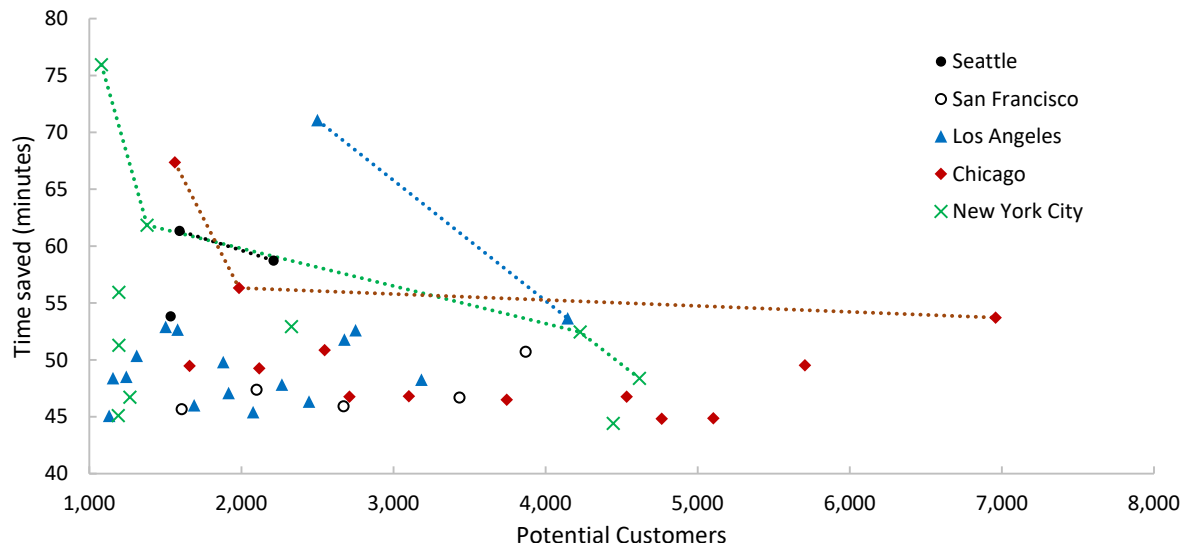


Fig. 6 Total number of potential customers and the associated average time saved for all airport pairs with 1000+ customers and 40+ minutes of time saved.

The dashed lines in Fig. 6 represent the Pareto fronts of airport pairs for each city, i.e. the airport pairs that maximize both the number of potential customers and the associated time savings. As can be observed, different cities dominate the Pareto frontier at different locations within the design space of Fig. 6. New York City has the routes with the highest time savings at lower customer numbers, Chicago does best if a higher number of customers is required, and Los Angeles performs well in between the two extremes. The city of San Francisco does not have a line associated to a Pareto front in Fig. 6 because only one airport-pair satisfied the filtering requirements.

Although the selected cities demonstrate a large number of potential customers for commuting trips, it is important to note that only a small fraction of these potential customers are expected to be willing to use the service. The number of potential customers, for example, that have historically commuted to work by car without carpools and earn over \$75,000 annually only represent about 10-20% of the total population. The anticipated demand for this more restrictive group of customers is shown in Fig. 7, where the number of potential customers per route can be seen to have reduced by an order of magnitude. New York City, which contains several of the country's highest median-income counties [24], shows a marked improvement with this subset of the population and claims a large portion of the Pareto front in Fig. 7.

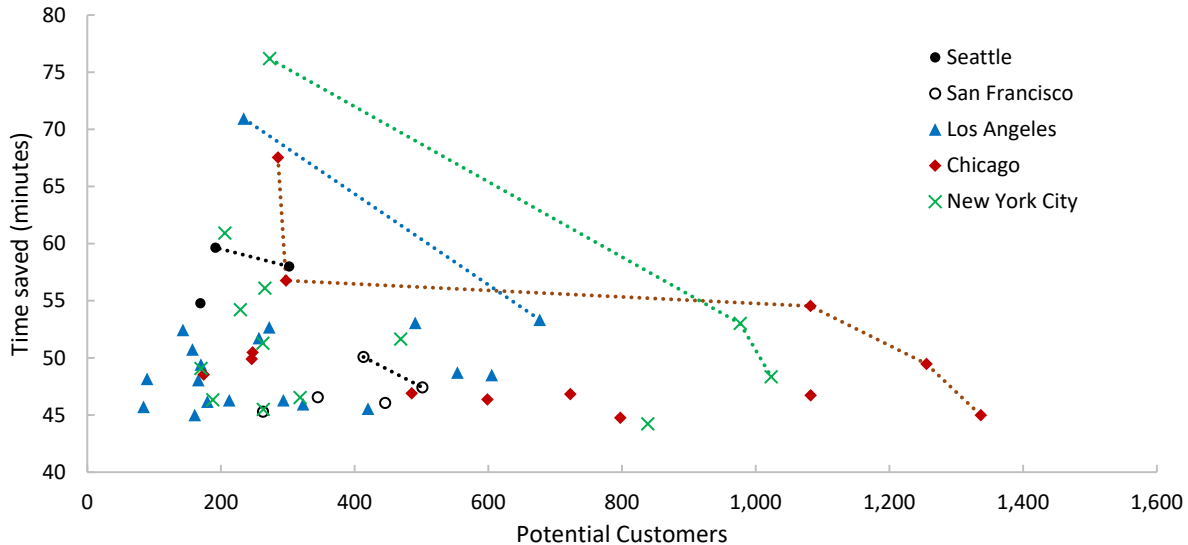


Fig. 7 Number of potential customers who drive alone and earn above \$75,000 and the associated time saved for all airport pairs with 1000+ customers and 40+ minutes of time saved.

The non-conflicting airport pairs plotted in Figs. 6 and 7 are mapped in Figs. 8 to 12, such that the location of each airport pair of interest and its associated catchment zone can easily be identified. The red circles in Figs. 8 to 12 represent the near-home airport locations used by commuters on their way to work from home, the blue circles denote the near-work airport locations, and the black lines connecting the home and work airport pairs illustrate which airports are linked as OD pairs. The shaded polygons surrounding each of the airports approximate the catchment zone of the airports, or in other words, approximates the area around each airport where customers using the service have a minimum time savings of 40 minutes. The diameter of the circles in Figs. 8 to 12 characterizes the number of potential customers for that airport pair, with a larger diameter denoting a higher number of potential customers. The opacity of the circles characterizes the associated average time saved by commuters of the airport pair, with a higher opacity denoting increased time savings.

Fig. 8 shows results for Seattle. As can be expected, the routes of interest are those where commuters would otherwise need to drive all the way around the peninsula or resort to ferry routes to reach their workplace or household destinations. The large bodies of water which isolate a significant number of people and feature no bridges make Seattle an ideal city for the proposed mission. The geographical layout of the city also has the advantage of allowing aircraft to fly the majority of their routes over water, thereby alleviating community noise concerns. It is also notable that Helijet, the largest operator of scheduled helicopter flights, which already offers helicopter services competing with cars, ferries, and conventional seaplanes in the Vancouver area, is currently considering leveraging electric aircraft to open a hub in Seattle for short range commutes [25]. The identification of Seattle as a candidate city for near-term routes both by the methodology described in this paper and by a commercial helicopter operator further supports conclusions regarding the suitability of routes in Seattle.

San Francisco, depicted in Fig. 9, also features a large body of water that separates populated regions and behaves similarly to Seattle. The presence of several bridges negates the need for ferry routes, leading to smaller time savings relative to Seattle. The bridges, however, become heavily congested during peak traffic hours and force many commuters who are crossing the San Francisco Bay to take a more non-linear commute path, thereby still allowing for reasonable time savings.

Although Los Angeles, shown in Fig. 10, benefits much less from geographical features than Seattle or San Francisco (using on the defined metrics), with the Angeles National Forest being the only exception, the considerable traffic congestion present in the city allows for significant time savings of 50-60 minutes, and the high density of the city gives rise to large customer bases per airport pair. One unique attribute of Los Angeles is the existence of airport pairs that have almost identical anticipated demand in both directions at a given time, shown by the existence of both blue and red circles of similar size and opacity on connecting airport pairs. Such routes have the advantage of requiring significantly fewer dead-head (empty) flights during the morning and evening commuting periods, thereby increasing potential profitability.

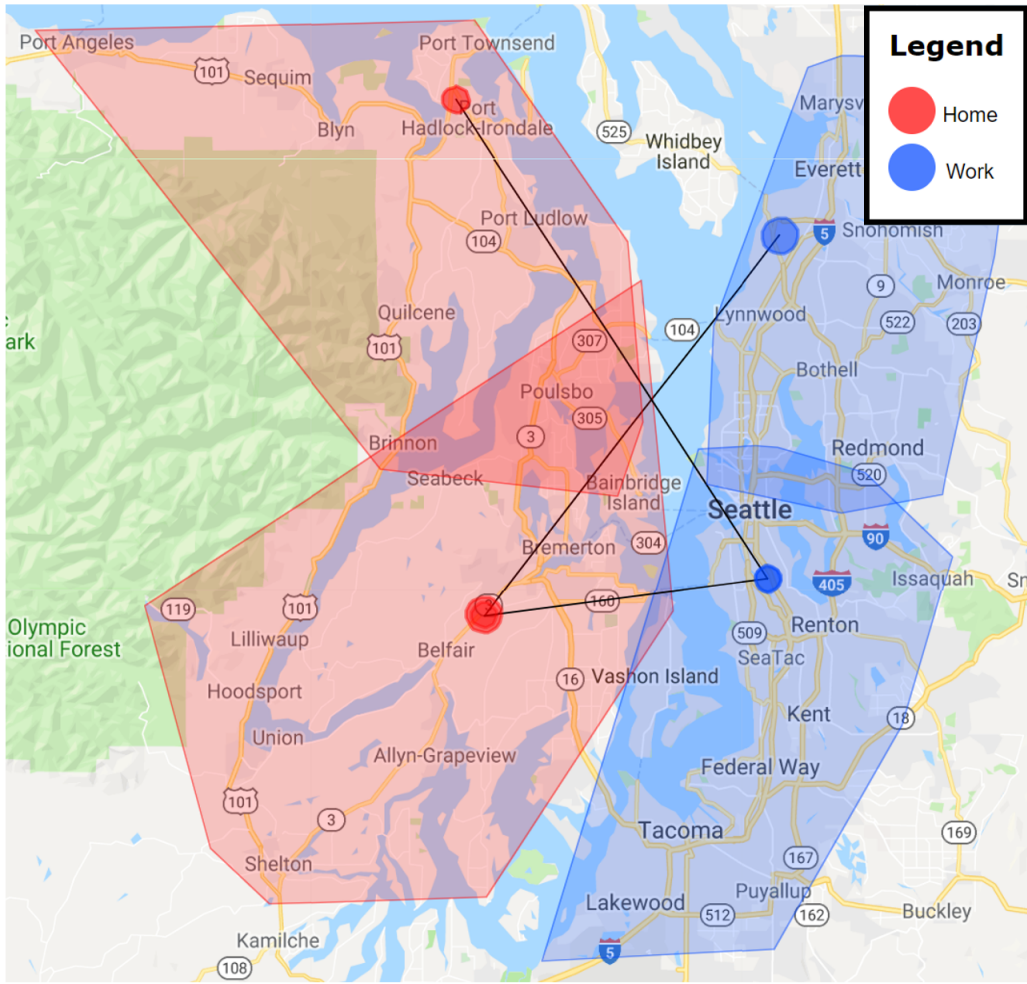


Fig. 8 Non-conflicting airport pairs and associated catchment zones for Seattle.

Similarly to Los Angeles, Chicago (Fig. 11) benefits minimally from geographical features, with Lake Michigan having little effect since cross-lake commuting demand is minimal. The square, grid-like nature of Chicago's roads, however, adds a significant distance penalty to ground commutes relative to the overflight distance. This, in conjunction with the high population density of Chicago, the large number of airports in the region, and the city's heavy traffic makes Chicago a suitable area of operations for the proposed mission.

New York City, shown in Fig. 12, follows many of the same trends as the cities described above. Routes which require commuting around the Long Island Sound or crossing the high traffic congestion surrounding the Manhattan area feature high time savings. The suitability of New York City is not surprising given the past operation of intracity helicopter services and the current success of BLADE, which, as part of their operations offer inter-airport helicopter transport services in NYC [4].

Given the near-term focus of the proposed mission, it is possible that only a single airport pair within the selected cities is of interest. Results for the top-ranked pair (based on the number of potential customers) of each city are provided in Fig. 13, with the Chicago Midway International Airport–Joliet Regional Airport pair showing the largest number of potential customers and significant time savings. Depending on the desire for possible expansion of operations, the number of aircraft in service, and depending on the fraction of the potential customers who are actually willing and able to use the service, it may be beneficial to select a route with fewer potential customers and a higher associated time savings. Time savings for most routes, including the aforementioned airport pair in Chicago, can be increased by restricting the customer base to OD pairs with higher time savings. The above analysis confirms the results from the nationwide analysis and demonstrates that a significant time benefit to customers exist from the use of an intracity air-transport service, particularly in the cities of Seattle, San Francisco, Los Angeles, Chicago, and New York City.

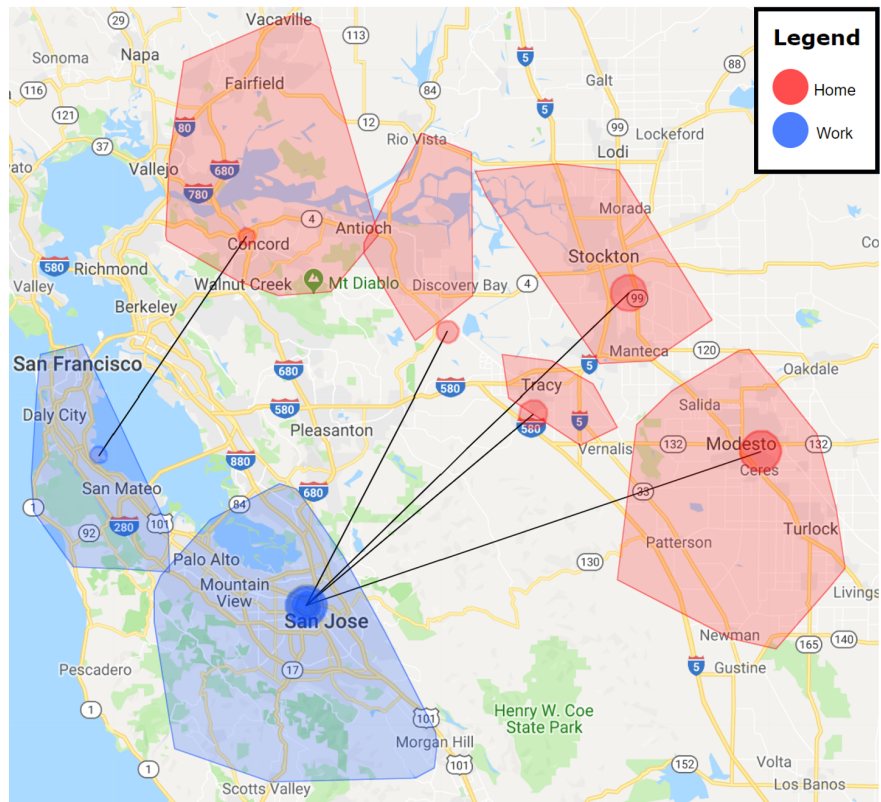


Fig. 9 Non-conflicting airport pairs and associated catchment zones for San Francisco.

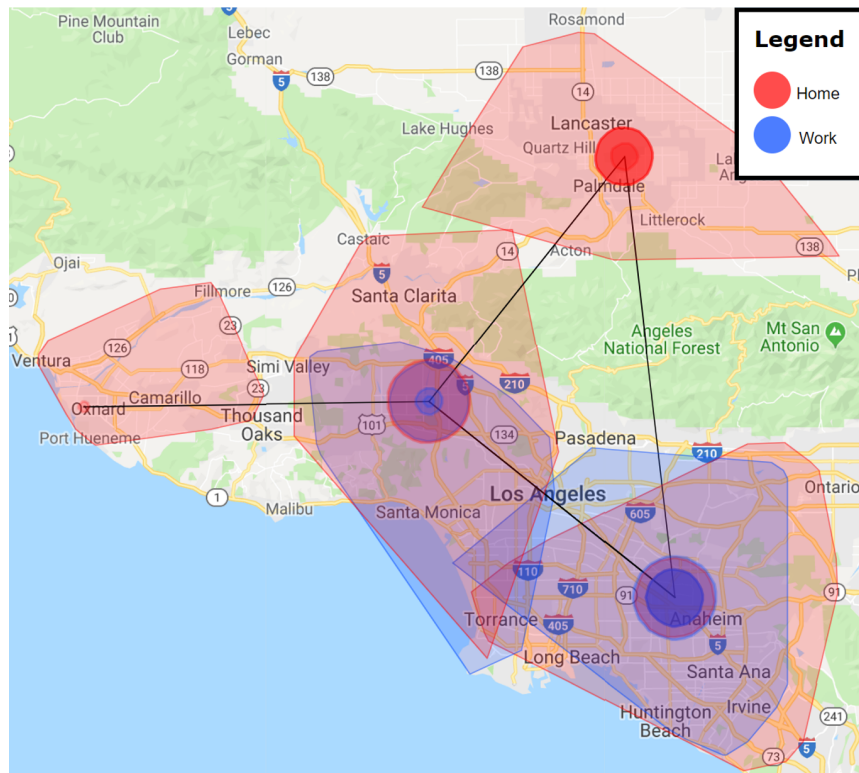


Fig. 10 Non-conflicting airport pairs and associated catchment zones for Los Angeles.

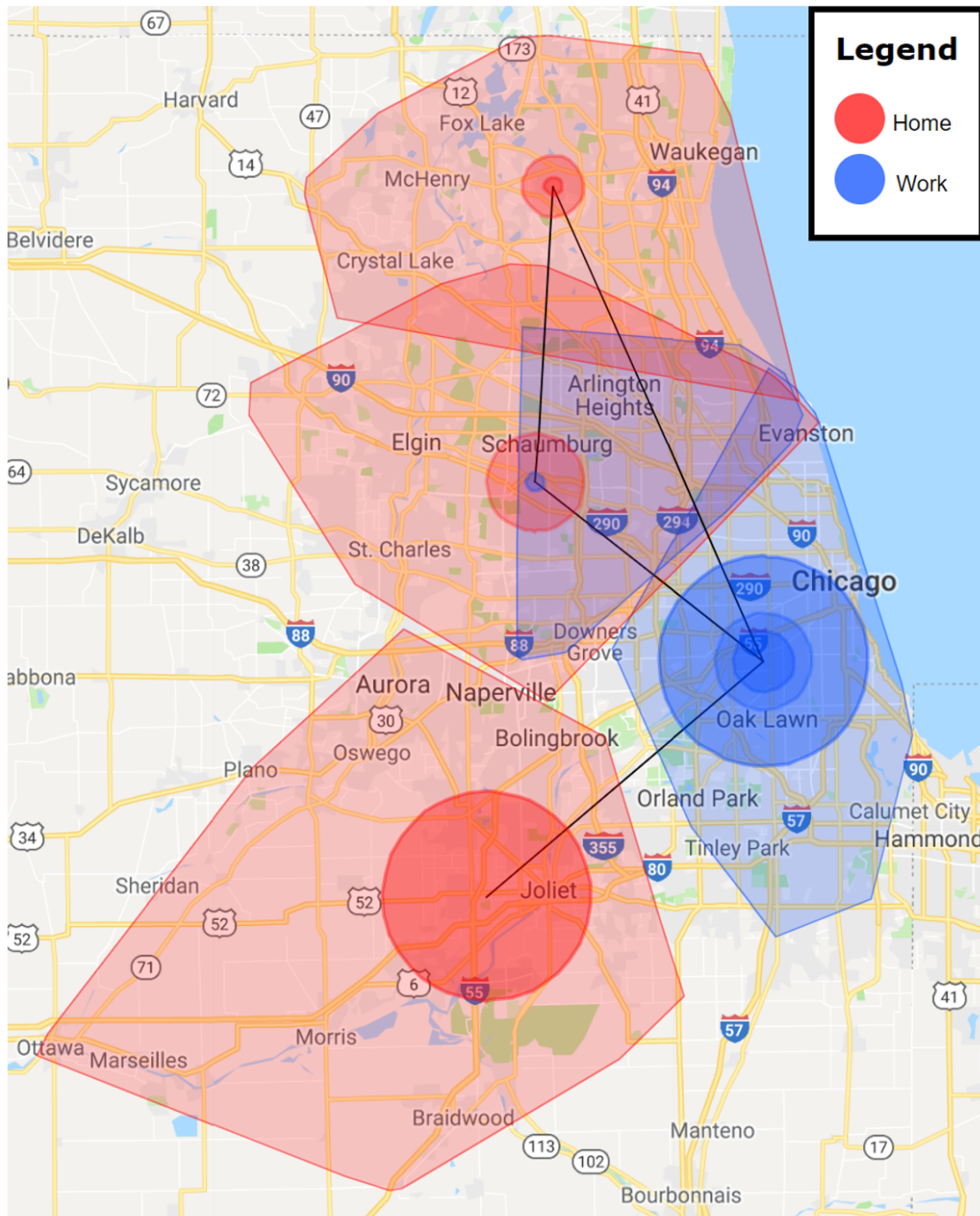


Fig. 11 Non-conflicting airport pairs and associated catchment zones for Chicago.

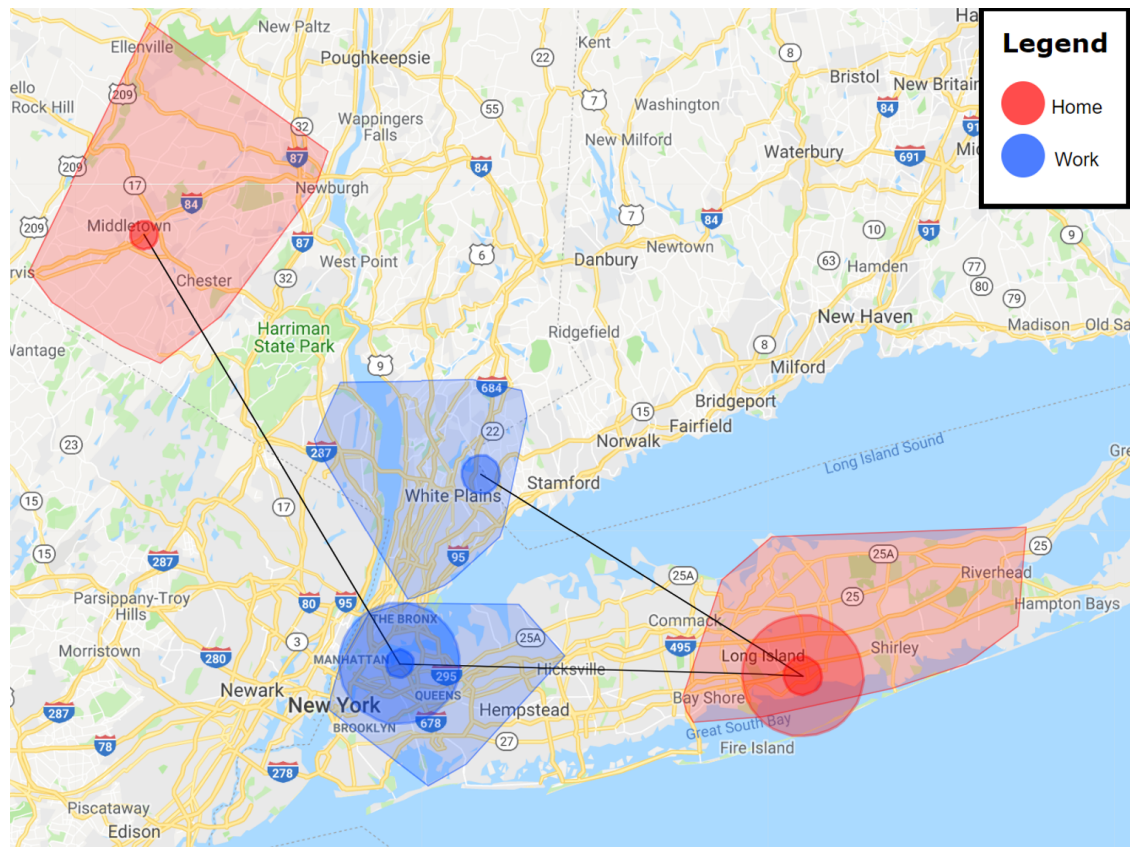


Fig. 12 Non-conflicting airport pairs and associated catchment zones for New York City.

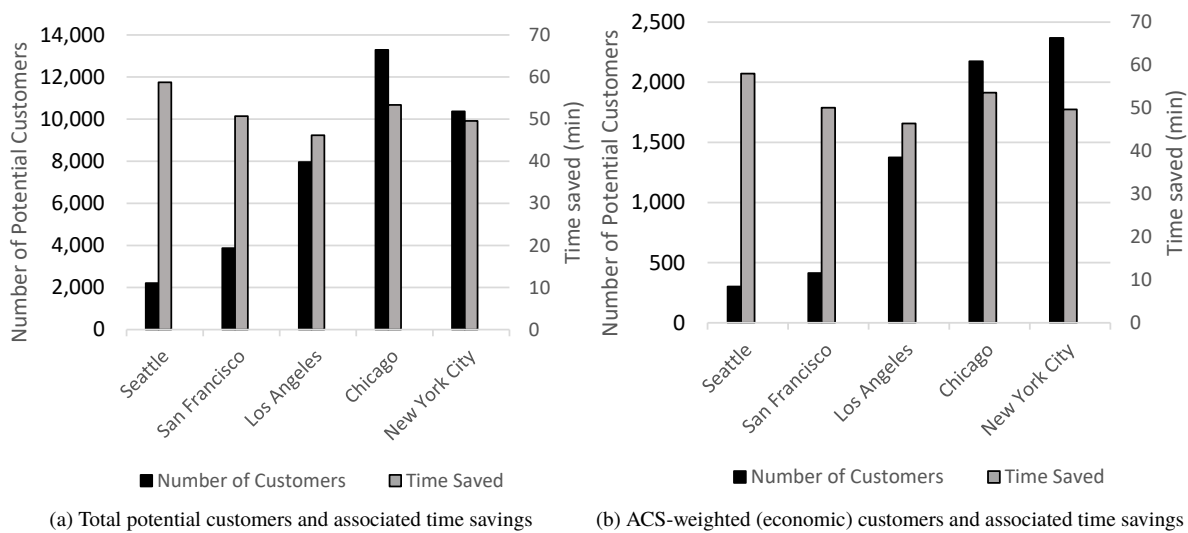


Fig. 13 Potential customers and time savings for single airport pair within top-ranked cities.

IV. Conclusion

The use of Cessna 208B Caravans retrofitted with electric propulsion systems proposed in this paper provides a new intracity transportation mode and has the potential to serve as a minimum viable product for the developing UAM market. The performance of a retrofitted Cessna 208B was modeled, and a range of 50 nautical miles at a cruise speed of 150 knots was determined to be feasible with current or near-term battery technology. A methodology was developed using the publicly accessible LODES and ACS datasets to identify the potential demand at the nationwide and city scale for the proposed mission. Using this methodology, the following conclusions can be made:

- The adopted nationwide methodology is capable of guiding the selection of regions of interest without use of traffic data by identifying densely populated zones with inefficient road networks (where the flyover distance is significantly shorter than the road network). Commuter origin-destination pairs across bodies of water that are currently served by ferry routes (such as Seattle) can also be identified.
- The adopted citywide methodology is capable of taking road traffic congestion into consideration and estimating anticipated mission time savings during peak traffic hours, providing an indication of the value proposition of the mission to customers.
- Results from this paper suggest that the proposed mission may be a viable near-term option for answering important questions about the UAM market and has the potential to provide a new transportation mode for customers in several cities.
- Significant and widespread demand was identified in several cities with Seattle, San Francisco, Los Angeles, Chicago, and New York demonstrating the highest potential customer demand and mission value potential. If only a single airport pair (per city) is of interest, the airport pair between Chicago Midway International Airport and Joliet Regional Airport in the city of Chicago is predicted to feature the highest number of potential customers.

Acknowledgments

The work has been supported by NASA through National Institute of Aerospace (NIA) task order 601048 under contract number NNL13AA08B.

References

- [1] MIT Flight Transportation Laboratory, “Concepts studies for future intracity air transportation systems,” Technical Report, Massachusetts Institute of Technology, Cambridge, MA, 1970. URL <http://dspace.mit.edu/handle/1721.1/68000>.
- [2] The Port of New York Authority, *Transportation by Helicopter, 1955-1975; a Study of Its Potential in the New Jersey-New York Metropolitan Area.*, New York., 1952. URL <http://hdl.handle.net/2027/mdp.39015006060837>.
- [3] Byrnes, M., “When Airport Hopping in New York Was Cheaper, Faster, and a Little More Dangerous,” , Aug. 2013. URL <https://www.citylab.com/transportation/2013/08/when-airport-hopping-new-york-was-cheaper-faster-and-little-more-dangerous/6652/>.
- [4] Goldstein, M., “Blade Puts Helicopter Or Fixed-Wing Flight Just An App Away,” , Aug. 2018. URL <https://www.forbes.com/sites/michaelgoldstein/2018/08/21/blade-puts-helicopter-or-fixed-wing-flight-just-an-app-away/>.
- [5] Airbus Helicopters, “Voom Joins Airbus Helicopters,” , Feb. 2019. URL <https://www.airbus.com/newsroom/press-releases/en/2018/02/voom-joins-airbus-helicopters.html>.
- [6] Garrow, L. A., German, B., Mokhtarian, P., Daskilewicz, M., Douthat, T. H., and Binder, R., “If You Fly It, Will Commuters Come? A Survey to Model Demand for eVTOL Urban Air Trips,” *2018 Aviation Technology, Integration, and Operations Conference*, AIAA AVIATION Forum, American Institute of Aeronautics and Astronautics, 2018. doi:10.2514/6.2018-2882.
- [7] Textron Aviation, “Grand Caravan,” , 2019. URL <https://cessna.txtav.com/en/turboprop/caravan>.
- [8] Garvey, W., Salerno, J. A., and McMillin, M., “MagniX Promises Electric Motor For Cessna 208 Caravan,” , Jun. 2018. URL <https://aviationweek.com/business-aviation/magnix-promises-electric-motor-cessna-208-caravan>.
- [9] Horne, T., “Pipistrel Alpha Electro: The Trainer of the Future?” , 2015. URL https://www.aopa.org/news-and-media/all-news/2015/october/pilot/f_pipistrel.
- [10] Moore, J., “Learning to train with electric airplanes,” , Apr. 2018. URL <https://www.aopa.org/news-and-media/all-news/2018/april/19/learning-to-train-with-electric-airplanes>.

- [11] Patterson, M. D., German, B. J., and Moore, M. D., “Performance Analysis and Design of On-Demand Electric Aircraft Concepts,” *12th AIAA Aviation Technology, Integration, and Operations (ATIO) Conference and 14th AIAA/ISSMO Multidisciplinary Analysis and Optimization Conference*, Aviation Technology, Integration, and Operations (ATIO) Conferences, American Institute of Aeronautics and Astronautics, 2012. doi:10.2514/6.2012-5474, URL <https://arc.aiaa.org/doi/10.2514/6.2012-5474>.
- [12] Moore, M. D., and Fredericks, B., “Misconceptions of Electric Aircraft and their Emerging Aviation Markets,” *52nd Aerospace Sciences Meeting*, AIAA SciTech Forum, American Institute of Aeronautics and Astronautics, 2014. doi:10.2514/6.2014-0535, URL <https://arc.aiaa.org/doi/10.2514/6.2014-0535>.
- [13] Magnusson, A., “Harbour Air Selects magniX to Transition to All-Electric Aircraft Fleet,” 2019. URL <https://apex.aero/2019/03/26/harbour-air-selects-magnix-electric-aircraft-fleet>.
- [14] Reuters, “Norway’s OSM Aviation Orders 60 Electric Planes to Cut Training Costs,” 2019. URL <https://www.nytimes.com/reuters/2019/04/11/technology/11reuters-norway-airplane-electric.html>.
- [15] Cessna Aircraft Company, “Information Manual Grand Caravan,” , 2008. URL www.redskyventures.org/doc/cessna-poh/Cessna_208_C208B-G1000_Grandcaravan_POH-PIM_2008.pdf.
- [16] Gunston, B., and Group, J. I., *Jane's Aero-engines*, JANE'S AERO ENGINES, Jane's Information Group, 1996. URL <https://books.google.com/books?id=1IU-QAAACAAJ>.
- [17] EMRAX, “User’s Manual for Advanced Axial Flux Synchronous Motors and Generators,” , 2016. URL https://emrax.com/wp-content/uploads/2017/01/emrax_348_technical_data_4.5.pdf.
- [18] Siemens, “World-record electric motor makes first flight,” , Jul. 2016. URL <https://www.siemens.com/press/PR2016070333COEN>.
- [19] Magnix, “Products,” , 2019. URL <https://www.magnix.aero/products/>.
- [20] Administration, F. A., “14 CFR § 91.151 - Fuel requirements for flight in VFR conditions,” , 2008. URL <https://www.law.cornell.edu/cfr/text/14/91.151>.
- [21] “Open data,” , 2019. URL <http://ourairports.com/data/>.
- [22] Warren, M., Garbo, A., Kotwicz Herniczek, M. T., Hamilton, T., and German, B., “Effects of Range Requirements and Battery Technology on Electric VTOL Sizing and Operational Performance,” *AIAA Scitech 2019 Forum*, 2019, p. 0527.
- [23] NEXA Advisors, “URBAN AIR MOBILITY - ECONOMICS AND GLOBAL MARKETS,” Tech. rep., NEXA, 2018.
- [24] “American Community Survey 5-Year Data (2009-2017),” , 2010. URL <https://www.census.gov/data/developers/data-sets/acs-5year.html>.
- [25] Vertical Flight Society, “The Electric VTOL Industry Shifts Gears,” , Apr. 2019. URL <http://evtol.news/2019/04/24/the-electric-vtol-industry-shifts-gears/>.